

Estimation of relative phycoerythrin concentrations from hyperspectral underwater radiance measurements—A statistical approach

Bettina B. Taylor,¹ Marc H. Taylor,¹ Tilman Dinter,² and Astrid Bracher^{1,2}

Received 22 August 2013; revised 11 April 2013; accepted 15 April 2013.

[1] Phycobiliproteins are a family of water-soluble pigment proteins that play an important role as accessory or antenna pigments and absorb in the green part of the light spectrum poorly used by chlorophyll *a*. The phycoerythrins (PEs) are one of four types of phycobiliproteins that are generally distinguished based on their absorption properties. As PEs are water soluble, they are generally not captured with conventional pigment analysis. Here we present a statistical model based on in situ measurements of three transatlantic cruises which allows us to derive relative PE concentration from standardized hyperspectral underwater radiance measurements (L_u). The model relies on Empirical Orthogonal Function (EOF) analysis of L_u spectra and, subsequently, a Generalized Linear Model with measured PE concentrations as the response variable and EOF loadings as predictor variables. The method is used to predict relative PE concentrations throughout the water column and to calculate integrated PE estimates based on those profiles.

Citation: Taylor, B. B., M. H. Taylor, T. Dinter, and A. Bracher (2013), Estimation of relative phycoerythrin concentrations from hyperspectral underwater radiance measurements—A statistical approach, *J. Geophys. Res. Oceans*, 118, doi:10.1002/jgrc.20201.

1. Description of Phycoerythrins

[2] The phycobiliproteins, a group of water-soluble, brightly colored proteins, are the major light-harvesting pigments of cyanobacteria, red algae and cryptophytes [Sidler, 1994; Zhao *et al.*, 2011]. They consist of open-chain tetrapyrroles known as phycobilins or bilins, that are covalently bound to the apoproteins via thioether bonds and they efficiently absorb light in the green part of the light spectrum poorly used by chlorophyll *a* (chl *a*) [French and Young, 1952; Glazer *et al.*, 1982; Kronick, 1986]. The colors of the phycobiliproteins originate mainly from the tetrapyrrole chromophores [Sidler, 1994]. In intact cells of cyanobacteria and chloroplasts of red algae, the phycobiliproteins are generally assembled in structures called phycobilisomes which are attached in regular arrays to the external surface of the thylakoid membranes [Gantt and Conti, 1966; Glazer, 1988; Sidler, 1994].

[3] Phycobiliproteins are usually classified according to their spectral properties and phylogenetic occurrence, although the classifications are constantly revised and discussed in the literature due to great spectral diversity and variation [e.g., Glazer, 1999; Hill and Rowan, 1989; Sidler,

1994; Six *et al.*, 2007; Zhao *et al.*, 2011]. In addition to the covalently bound chromophores, several noncovalent interactions between the apoprotein and the chromophores are essential for the light-harvesting function and influence the spectral properties of the proteins. Generally, four types of phycobiliproteins are distinguished on the basis of their absorption maxima (Abs_{max}): phycoerythrocyanins (PEC, $Abs_{max} \sim 575$ nm), phycoerythrins (PE, $Abs_{max} \sim 495$ – 575 nm), phycocyanins (PC, $Abs_{max} \sim 615$ – 640 nm) and allophycocyanins (APC, $Abs_{max} \sim 650$ – 655 nm). Cryptophyte biliproteins are often classified as a separate group. In this paper, we will concentrate on the PEs.

[4] PEs carry only one or two chromophore types, phycoerythrobilin (PEB, $Abs_{max} \sim 545$ nm) and phycourobilin (PUB, $Abs_{max} \sim 495$ nm). They exhibit very diverse spectral characteristics depending on their molecular structure which varies among phytoplankton species and with environmental conditions such as light and nutrient availability [Haverkamp *et al.*, 2009; Hoge *et al.*, 1998; Lantoiné and Neveux, 1999; Palenik, 2001; Sidler, 1994]. The spectral characteristics of PEs are strongly influenced by the number and proportions of PUB and PEB, the chemical structure and geometry of the molecule, and their direct local environment, which can lead to varying absorption maxima [MacColl, 1998]. PEB is found in all PEs, whereas PUB is present in varying concentrations in some forms of PE [Glazer, 1999; Six *et al.*, 2007; Wood *et al.*, 1998]. Generally, species with high-PUB content are more abundant in clear oligotrophic waters of the open ocean, whereas low-PUB or no-PUB PEs characterize species that are native in more eutrophic coastal waters [Chekalyuk and Hafez, 2008; Lantoiné and Neveux, 1999; Wood *et al.*, 1998]. PEs generally have a single fluorescence emission

¹Alfred Wegener Institute for Polar and Marine Research, Bremerhaven, Germany.

²Institute of Environmental Physics, University of Bremen, Bremen, Germany.

Corresponding author: B. B. Taylor, Department of Climate Dynamics, Alfred Wegener Institute for Polar and Marine Research, Bussestrasse 24, Bremerhaven D-27570, Germany. (Bettina.Taylor@awi.de)

maximum regardless of the presence or absence of PUB, indicating that only PEB chromophores fluoresce, although the presence of PUB can influence the emission wavelength of PEB. PEB fluorescence peaks at ~ 580 nm, but can be shifted to shorter wavelengths for PUB-containing PEs [Chekalyuk and Hafez, 2008; Falkowski and Raven, 1997; Hoge et al., 1998; Lantoiné and Neveux, 1997; Ong and Glazer, 1991].

1.1. Phycoerythrins in the Marine Environment

[5] Our understanding of the functioning of marine ecosystems starts with the phytoplankton because of their fundamental role in the marine food web and carbon cycle. PE-containing species of the phytoplankton are a globally important group of photosynthetic organisms and are distributed ubiquitously throughout oceanic regions, ranging from polar through temperate to tropical waters in coastal and open ocean regions [Hoef-Emden, 2008; Partensky et al., 1999; Scanlan and West, 2002; Wood et al., 1998]. Within the picophytoplankton (cells $< 2 \mu\text{m}$), the PE-rich cyanobacteria are a widely recognized and studied phytoplankton group in the marine environment [Carr and Mann, 1994; Everroad and Wood, 2012; Partensky et al., 1999; Scanlan and West, 2002]. They have been shown to be important primary producers; species of the genus *Synechococcus*, for example, have been estimated to account for 64% of total photosynthesis in the North Pacific [Iturriaga and Mitchell, 1986]. Other picocyanobacterial strains such as a PE-containing *Cyanobium*, a *Cyanobium*-like lineage and species of the genus *Synechocystis* can occur alongside *Synechococcus* in open ocean areas [Everroad and Wood, 2006; Waterbury and Rippka, 1989]. Another important PE-containing genus is *Trichodesmium*, a group of filamentous cyanobacteria that forms extensive colonies in surface waters of oligotrophic, tropical and subtropical oceans [Capone et al., 1997; Staal et al., 2007; Subramaniam et al., 1999]. The two eukaryotic PE-containing groups (cryptophytes and red algae) are more prevalent in coastal, brackish, and freshwater environments; red algae occur mainly as macroalgae [Clay et al., 1999; Cole and Sheath, 1990; Gabrielson et al., 1989; Gillot, 1989; Hoef-Emden, 2008].

1.2. Challenges of Phycoerythrin Measurement

[6] PEs seem to be ideal marker pigments for PE-containing cyanobacteria. However, contrary to all other algal pigments which are soluble in organic solvents, measurements of phycobiliproteins are still scarce. A number of methods have been proposed to measure PEs in water samples [e.g., Algarra et al., 1988; Downes and Hall, 1998; Kim et al., 2011; Lantoiné and Neveux, 1997; Ong et al., 1984] or in vivo [Beutler et al., 2002; Chekalyuk and Hafez, 2008; Chekalyuk et al., 2012; Cowles et al., 1993; Hoge et al., 1998], but none are routinely used in oceanography, thus leaving PEs often undetected in pigment analysis. The most commonly used method, which detects PEs through its orange fluorescence, is flow cytometry. Nevertheless, these methods need discrete water samples and involve a certain amount of, often complex and time consuming, sample preparation. Very detailed information about spatial and spectral variability and distribution of PEs without the need of discrete water samples can be

obtained from methods such as laser-induced emission measurements from airborne platforms [Hoge et al., 1998] or as shipboard-device [Chekalyuk and Hafez, 2008; Chekalyuk et al., 2012]. However, these measurements require very sophisticated instrumentation that is not easily acquired and handled and have been confined to underway surface measurements or water samples from discrete depths. Automated submersible flow cytometers have been developed [Dubelaar et al., 1999; Olson et al., 2003] and used as moored devices measuring time series, but, as far as we are aware, not for profiling. Some submersible and profiling fluorometers exploiting the fingerprints of the specific excitation spectra of PE-containing phytoplankton have been designed [Beutler et al., 2002, 2004; Cowles et al., 1993; Desiderio et al., 1997; Horiuchi and Wolk, 2008] and some of these PE fluorometers are commercially available. These profiling fluorometers have been mainly deployed in freshwater environments [Beutler et al., 2002; Leboulanger et al., 2002; Proctor and Roesler, 2010]. Thus, even though PEs and PE-containing phytoplankton have been subject to many studies, there is still a lack of information about the depth distribution in marine ecosystems and the deep maxima are often overlooked. Here we demonstrate a method which deduces profiles of total PE down to the depth of measurable light availability.

[7] The spectral diversity of the PEs opens many possibilities to distinguish between PE-containing groups as has been shown with many of the methods mentioned above, but also carries many difficulties, when only specific wavelengths are used for the excitation and detection of the different groups. Ample research has shown that PE content and spectral properties can vary with light availability (thus also with depth) and nutrient status [Lantoiné and Neveux, 1999; Wood et al., 1998; Wyman et al., 1985]. For example, in some species PE is not only used in photosynthesis, but also as nitrogen storage [Wyman et al., 1985]. All the methods mentioned above use some kind of fluorescence excitation to detect PEs; some methods use only one excitation and emission wavelength (for example many flow cytometers), others use several excitation and/or emission wavelengths to distinguish between spectral varieties of PE. As input parameter into our model, we use PE values, determined by a method that takes the whole diversity of PEs into account and thus, on the expense of losing the information about specific spectral types of PE, measures total PE.

[8] Building on the fact that PE absorption and fluorescence have an impact on the underwater light field, we propose a statistical method that allows for the prediction of relative PE concentrations from underwater upwelling radiance (L_u) measurements. Several studies have shown that PE-containing phytoplankton influence the submarine light field due to absorption, scattering and fluorescence processes [Hoge and Swift, 1990; Kirk, 1986; Morel, 1997]. Taking advantage of this fact, we apply Empirical Orthogonal Function (EOF) analysis to decompose a matrix of corresponding L_u spectra, as this method has been shown to be particularly useful for assessing variance structure in spectral measurements such as remote sensing reflectance [Craig et al., 2012; Lubac and Loisel, 2007; Mueller, 1976; Toole and Siegel, 2001]. So far, the idea to retrieve information about pigments from radiometric data has been

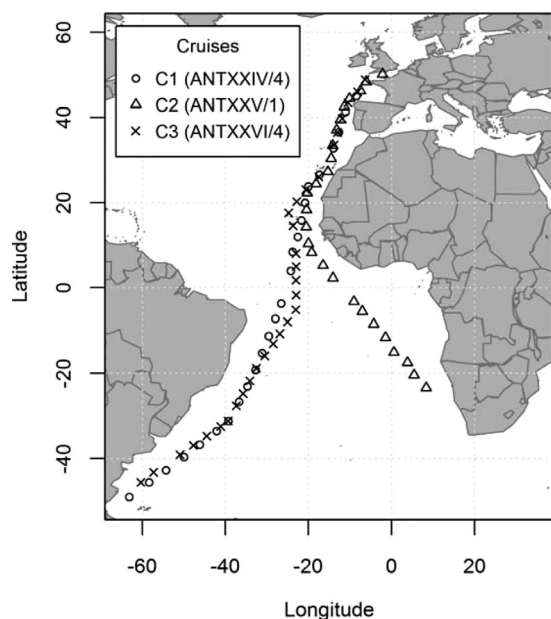


Figure 1. Map of the Atlantic Ocean with tracks of the three cruises. Points show all stations where concurrent measurements of PE and L_u were conducted.

mainly applied to the main photosynthetic pigment chl *a* and has been successfully extended to retrieve global chl *a* concentrations from satellite data [e.g., Gordon *et al.*, 1980; McClain, 2009].

[9] The method presented here is used to predict PE profiles and values of integrated PE based on upwelling radiance spectra. The aim was to develop a method that can be easily applied to radiometric measurements and thus is applicable to measurements at all depths as long as light is detectable. With only a few discrete water samples and PE measurements, information about whole profiles of total PE can be extracted.

2. Methods

2.1. Sample Collection

[10] Samples were collected during three cruises: the ANT-XXIV/4 expedition of the RV Polarstern in April/May 2008 along a South-to-North transect through the Atlantic Ocean from Punta Arenas (Chile) to Bremerhaven (Germany), the ANT-XXV/1 expedition of the RV Polarstern in November 2008 along a North-to-South transect through the eastern Atlantic Ocean from Bremerhaven (Germany) to Cape Town (South Africa) and the ANT-XXVI/4 expedition of the RV Polarstern in April/May 2010 along a South-to-North transect through the Atlantic Ocean from Punta Arenas (Chile) to Bremerhaven (Germany). For convenience the cruises will be called C1 (ANTXXIV/4), C2 (ANTXXV/1) and C3 (ANTXXVI/4) (Figure 1). Sampling stations generally coincided once a day at noon local time and involved CTD casts with water samplers as well as above- and below-water radiance and irradiance measurements. Water samples were filtered on 0.4 μm polycarbonate filters for PE analysis and on GF/F filters for analysis of other pigments, shock-frozen in liquid nitrogen and stored at -80°C . Samples for flow cytometry were preserved with 0.1% glutaraldehyde (final

concentration), shock-frozen in liquid nitrogen and stored at -80°C . A total of 131 water samples were taken (26, 62, and 43 on C1, C2, and C3, respectively) and 59 radiance profiles were measured (13, 22, and 24 on C1, C2, and C3, respectively) at the same time as the water samples. At each station, we took at least two water samples at the surface and the chl *a* maximum; if possible a third sample was taken at 100 m.

2.2. Phycoerythrin Measurements

[11] PE measurements were based on the *in vivo* method by Wyman [1992] and the spectrofluorometric assay by Lantoiné and Neveux [1997] and Neveux *et al.* [2006]. In detail, the polycarbonate filters were placed into 3 ml of 50/50 mixture of glycerol and phosphate buffer (0.1 mol L^{-1} NaH_2PO_4 (pH = 6.5)) and the cells on the filters were resuspended by vigorous shaking on a lab bench vortex mixer. The choice of filters and buffer was made following extensive tests with different methods and personal communication with J. Neveux. Samples were kept on ice and in the dark for 1h and vortexed again before fluorescence was measured with a Fluorolog FL3–22 spectrofluorometer (Horiba). We performed an excitation scan from 450 to 560 nm (emission: 575 nm). Excitation slits were set to 5 nm. As we were not able to purify PEs for calibration purposes, our results remain relative values and could not be converted into absolute concentrations. The relative PE concentration per L seawater was calculated from the integrated area below the blank-subtracted excitation spectra between 450 and 560 nm. Spectra were normalized to the Raman scatter [e.g., Coble *et al.*, 1993; Seppälä *et al.*, 2005] and the fluorometer was equipped with a reference detector to monitor and compensate for variations in the xenon lamp output; thus even though the concentrations are relative, they are comparable between samples and cruises.

2.3. Pigment Analysis

[12] The composition of pigments which are soluble in organic solvents was analyzed by High Performance Liquid Chromatography (HPLC) following a method described by Hoffmann *et al.* [2006] adjusted to our instruments as detailed by Taylor *et al.* [2011].

2.4. Flow Cytometry

[13] Phytoplankton cells were enumerated from preserved and frozen, unstained samples by using their specific chl *a* and PE autofluorescence as described by Marie *et al.* [2005]. Flow cytometry was performed on a FACScalibur with an excitation beam of 488 nm, two light scatter detectors at 180° (forward scatter) and at 90° (side scatter) and several photomultipliers detecting at 530 ± 15 nm (green fluorescence), 585 ± 21 nm (orange fluorescence) and >670 nm (red fluorescence). Phytoplankton groups were separated according to their red and orange fluorescence and scattering characteristics. Yellow-green Fluoresbrite® Microspheres with a diameter of 1 μm (Polysciences) were used as an internal standard. The data were analyzed with the instrument software “CellQuest.”

2.5. Radiometric Measurements

[14] Underwater optical light fields were measured with hyperspectral radiometers (RAMSES, TriOS GmbH, Germany) measuring radiance profiles. The instrument covers a wavelength range of 320–950 nm with an optical

resolution of 3.3 nm and a spectral accuracy of 0.3 nm. All measurements were collected with sensor-specific automatically adjusted integration times (between 4 ms and 8 s). Radiometric profiles measuring upwelling radiance (L_u) [$\text{W m}^{-2} \text{nm}^{-1} \text{sr}^{-1}$] were collected at the same time as the CTD profiles on a second winch down to a maximum depth of 190 m. Irradiance at the surface (E_d^+) [W m^{-2}] was measured as a reference with a second sensor placed above-water and was utilized to normalize the measured under-water data to a maximum value of E_d^+ as described by *Smith and Baker* [1984]. The radiance sensor had a field of view of 7° , while the irradiance sensor had a cosine collector fixed in front of the instrument. The in-water sensor was equipped with an inclination and a pressure sensor. To avoid ship shadow, the ship was oriented such that the sun was illuminating the side where the measurements were taking place. The pitch and roll data measured by the ship did not exceed values larger than 5° . For the in-water data, the inclination in either dimension was smaller than 14° [*Matsuoka et al.*, 2007].

2.6. Statistical Methods

[15] We first processed the data of all cruises together, followed by the analysis of each cruise separately. As cruise C3 yielded different results than the two other cruises (possible reasons will be discussed below), we also analyzed a data set consisting of the data of cruises C1 + C2 only.

2.6.1. Empirical Orthogonal Function Analysis

[16] All analyses were conducted using the statistical computing software “R” [*R Development Core Team*, 2011]. Spectral data were subjected to an Empirical Orthogonal Function (EOF) analysis (sometimes referred to as Principal Component Analysis) in order to reduce the high dimensionality of the data and derive the dominant signals (“modes”) that best describe variance within the data set. We averaged the L_u spectra within one cast that were measured within ± 1 m depth of the respective discrete PE measurement. The sampling rate of the radiometer depended on integration time, which is affected by light availability. As a result, the number of sampled spectra decreased with depth and the number of spectra used for the average ranged from 3 to 10 samples. The averaged L_u spectra were used to create a data matrix \mathbf{X} consisting of M rows of L_u radiances, from 350–800 nm in 1 nm increments, by N sample columns. The resulting data matrix consisted of $M=451$ rows (nm), while the number of N columns (samples) varied between models. Prior to analysis, the L_u spectra were standardized by first subtracting the mean (centering) and then dividing by the standard deviation (scaling), in order that each spectral sample (columns) had a mean of zero and standard deviation of one (i.e., dimensionless). This standardization step allowed us to focus on spectral shape rather than magnitude. All results shown in this paper are from standardized spectra. Subsequently, a covariance matrix was calculated:

$$\mathbf{C} = \frac{1}{M} \mathbf{X}^T \mathbf{X} \quad C_{jl} = \overline{X_j X_l}. \quad (1)$$

[17] The covariance matrix \mathbf{C} was then subjected to an Eigen decomposition:

$$\mathbf{C} = \mathbf{E} \mathbf{\Lambda} \mathbf{E}^T \quad \mathbf{C} = \sum_{k=1}^N e_k \lambda_k e_k^T, \quad (2)$$

[18] with EOFs equaling the Eigenvectors \mathbf{E} , and $\mathbf{\Lambda}$ being a diagonal matrix containing the eigenvalues, by which the explained variance of each EOF can be calculated. \mathbf{E} is an $N \times N$ matrix containing loadings for each sample by mode. EOF expansion coefficients \mathbf{Z} (i.e., “principal components”) are then calculated as the projection of the data \mathbf{X} onto \mathbf{E} :

$$\mathbf{Z} = \mathbf{X} \mathbf{E} \quad Z_{ik} = \sum_{j=1}^N X_{ij} e_{jk}, \quad (3)$$

where \mathbf{Z} is an $M \times N$ matrix carrying the loadings for each radiance wavelength (nm) by mode.

2.6.2. Generalized Linear Model

[19] The number n of significant EOF modes was determined according to North’s Rule-of-Thumb [*North et al.*, 1982]. The significant EOF modes from \mathbf{E} were then used as covariates in the prediction of measured PE concentrations using a multiple Generalized Linear Model (GLM):

$$\log_e(E(PE)) = \alpha + \beta_1 e_1 + \beta_2 e_2 + \dots + \beta_n e_n, \quad (4)$$

where $e_{1,2,\dots,n}$ are the leading n significant EOF modes from \mathbf{E} , α is the intercept, and $\beta_{1,2,\dots,n}$ are the regression coefficients. The GLM assumed a Gaussian error distribution and used a log-normal link function for the expectation of PE, $E(PE)$. The model assumes that error dispersion is constant and independent of PE, which is consistent with the error of the method used to determine its concentration [*Lantoiné and Neveux*, 1997]. The log-link function GLM provided a better fit over that of a simple linear model (in terms of sum of squared differences) and also had the advantage of preventing the prediction of negative values.

[20] A stepwise routine was used to search for smaller models based on fewer terms, through minimization of the Akaike information criterion (AIC). Once the best model was determined, the significance of included terms was defined by the change in AIC (ΔAIC) following each term’s removal. This is an appropriate test for the comparison of nested models because it includes a penalty for the number of parameters in the model.

2.6.3. PE Prediction

[21] The model was applied to spectra from depths that did not have corresponding PE measurements in order to create profiles of estimated PE. This new set of radiance spectral data \mathbf{Y} was first projected onto the EOF domain using the EOF coefficients \mathbf{Z} :

$$(\mathbf{Z}^{-1} \mathbf{Y})^T = \mathbf{F}, \quad (5)$$

where \mathbf{F} is an $N \times N$ matrix giving the loadings for each sample, as with \mathbf{E} . Predicted PE is then calculated using the best fitted GLM and the new EOF loadings \mathbf{F} :

$$\log_e(E(\text{PE}_{\text{pred}})) = a + b\beta_1 f_1 + \beta_2 f_2 + \dots + b\beta_n f_n, \quad (6)$$

where PE_{pred} equals the predicted relative PE concentrations and $f_{1,2,\dots,n}$ are the EOF loadings \mathbf{F} that correspond to the significant terms of the multiple regression model

Table 1. Percent of Total Variance Explained by the Significant EOFs Derived from Radiance Spectra from Various Combinations of Cruise Data

Cruise	EOF1	EOF2	EOF3	EOF4	EOF5	EOF6	EOF7	EOF8	EOF9
C1	82.3	12.1	4.4	0.9	0.1				
C2	86.6	9.9	2.6	0.5	0.2	<0.1			
C3	81.0	13.0	5.2	0.5	0.1	<0.1	<0.1	<0.1	<0.1
C1+C2	85.1	10.6	3.2	0.6	0.2				
C1+C2+C3	83.5	11.4	4.1	0.6	0.2				

(equation (4)). Confidence intervals were calculated for each PE_{pred} based on the standard error of the GLM coefficients.

2.6.4. Integrated PE

[22] Using the above procedure, PE concentration was predicted from radiance spectra throughout each station's sampled profile. A spline function was fitted to the predicted values by depth and used for the calculation of integrated values for each profile (in relative PE concentration m^{-2}). In order to include a majority of stations in the comparison, integrated values were calculated down to a depth of 95 m, since most station profiles were sampled to at least this depth.

3. Results

3.1. EOF Analysis of L_u Spectra

[23] The decomposition of the standardized spectra by the EOF analysis returned between 5 and 9 significant EOFs explaining most of the variance of the data matrix (Table 1). Figure 2 illustrates the 3 dominant EOF coefficients for each of the cruises (for visual comparison, we have removed the eigenvalue units in order to present all coefficients on a similar scale). The shapes of these 3 EOF coefficients were similar in all analyses and explained most of the variance ($> 98\%$). EOF coefficients four to nine generally added less than 1% and thus are not discussed in detail in this paper. The gray area in the plots indicates the area where the main signal of PEs is to be expected due to their absorption and fluorescence features in the spectral range of 450–600 nm. EOF coefficient 1 shows positive

values in the wavelength region of 400–500 nm with no other conspicuous effects in the region above 550 nm. EOF coefficient 2 also showed main deviations (positive and negative) in the region of 400–500 nm, while EOF mode 3 showed a negative peak between 450 and 500 nm and positive values in the wavelength region of 500–600 nm.

3.2. Generalized Linear Models

[24] Figure 3 shows the predicted versus the measured PE values for each analysis. The models show better fits for data sets of individual cruises than when all cruises were grouped together. In particular, adding C3 to the model using only data from C1 and C2 lowered R^2 substantially, although the correlation was still highly significant at $p < 0.0001$. All cruises showed a large range of PE values; however C3 had very low-PE values compared to the two other cruises. Reasons for these variations will be discussed below.

[25] In order to estimate the importance of each EOF in the best model, we used the ΔAIC as a measure of each smaller model (without the respective EOF) relative to the best model. The bigger the ΔAIC , the greater the importance of the removed EOF (Table 2). In all models EOF 3 was the most significant predictor of PE concentrations.

3.3. PE Prediction

[26] Using the regression models we predicted PE profiles and integrated PE values from the radiance measurements. Figure 4 shows the integrated PE (relative concentration m^{-2}) for all stations of C1, C2, and C3 of which we had L_u profiles down to 95 m. The profiles were calculated with the models of the respective cruises and the

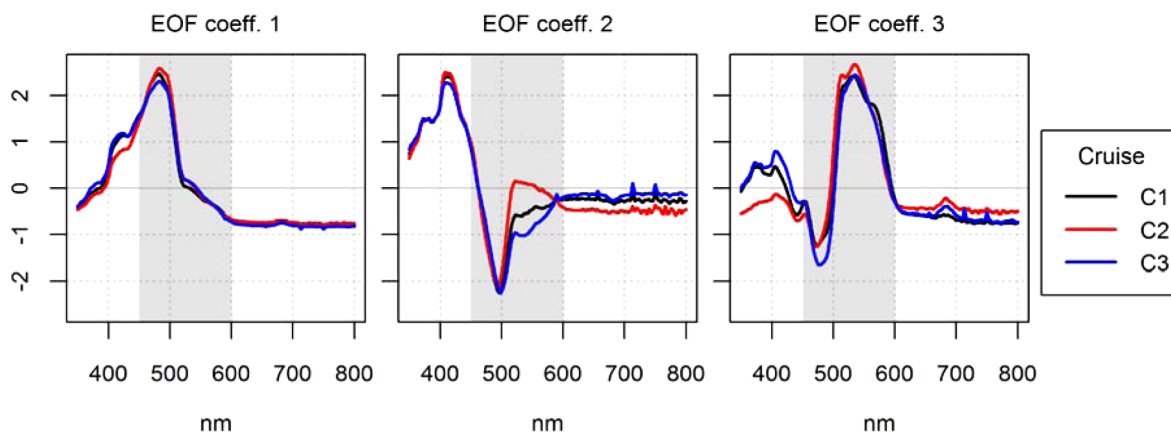


Figure 2. Leading three EOF coefficients (scaled) as calculated from the standardized L_u spectra for the single cruise models. Each cruise is designated by a color. The gray area indicates the wavelength range where the main influence of PEs is to be expected (450–600 nm).

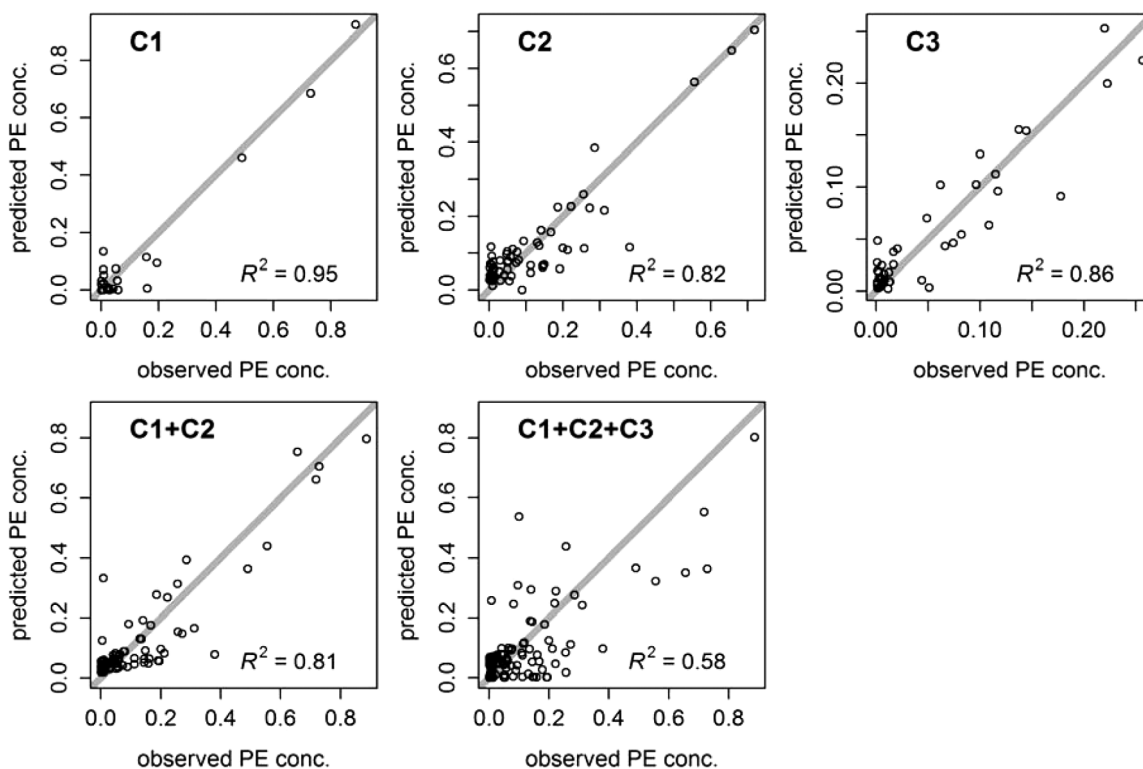


Figure 3. Observed versus predicted PE values for models based on various combinations of cruise data. All models are highly significant at $p < 0.0001$. The 1:1 line is shown in gray for reference.

gray areas around the profiles show the 95% confidence intervals of the predictions. The cumulative error of the multiple regression EOF terms increases the confidence interval for the higher range of predicted PE concentrations. Integrated PE values are highest in the Bay of Biscay, off the West coast of Portugal, in the Mauritanian upwelling and off the coast of Namibia. Seven example PE profiles from stations of different biogeographical regions of the Atlantic Ocean are depicted in the figure. The profiles show that PE distribution by depth can be very different, ranging from the main concentration residing in surface waters to deep maxima at >50 m. See Figure A1 in the Appendix for all predicted profiles.

4. Discussion

[27] EOF analysis is a statistical method that has proved useful in extracting information about water constituents from spectral data since the 1970s [Craig *et al.*, 2012; Lubac and Loisel, 2007; Mueller, 1976; Toole and Siegel, 2001]. Most authors used this method on ocean color re-

flectance data to derive information about chl *a*, particulate backscattering, nutrients or other biochemical or optical parameters. We have applied this method to upwelling underwater radiance in the hope to be able to use underwater light measurements for the estimation of pigment profiles which cannot be measured easily in the same resolution with common laboratory methods.

[28] PEs and PE-containing cyanobacteria have been studied extensively. Especially the genus *Synechococcus*, a group of small unicellular cyanobacteria with a wide geographical distribution and considerable impact on the global carbon cycle, has been the interest of many research projects since its discovery in the late 1970s [Waterbury *et al.*, 1979]. Most data on the depth distribution are still based on discrete water samples and laborious measurement techniques involving a great amount of sample preparation and instrumentation, thus often relying on a small number of samples only. More recently, some specific PE sensors have been developed, which estimate PE fluorescence using one or several excitation and emission wavelengths (see section 1.3.).

Table 2. Change in the Akaike Information Criterion (Δ AIC) Following Individual Term Removals from the Best Multiple Regression Models

Cruise	EOF1	EOF2	EOF3	EOF4	EOF5	EOF6	EOF7	EOF8	EOF9
C1			73	22					
C2		11	95	25	25	29			
C3	10	35	45				8	4	18
C1+C2	40		129						
C1+C2+C3	17	18	71	19					

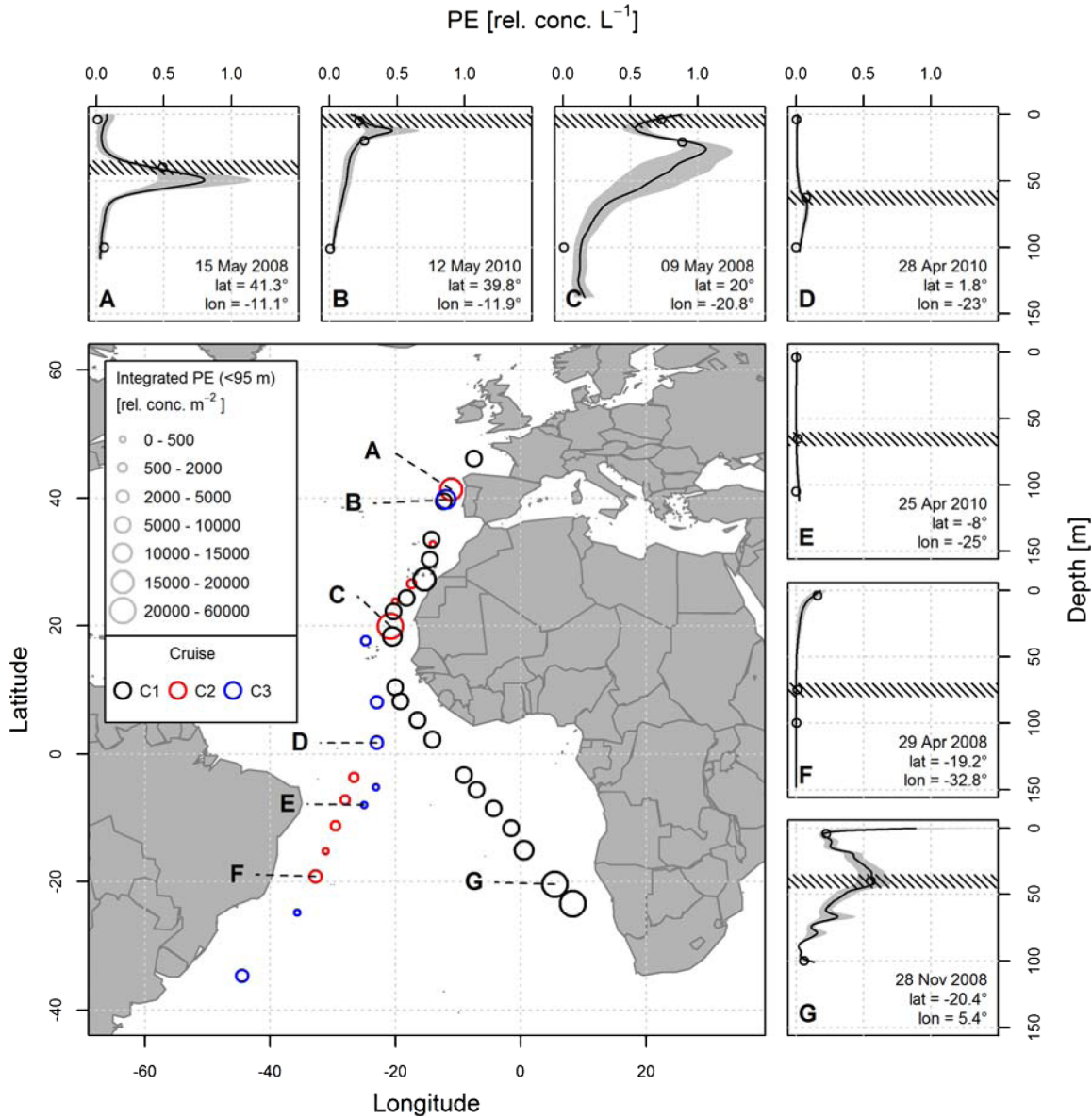


Figure 4. Map of the Atlantic Ocean with all stations of which a value of integrated PE could be calculated from the L_u profiles. The integrated values were calculated with the single cruise models. Each cruise is designated by a color. Arranged around the map are seven examples of predicted PE profiles, including the values of measured PE (open circles) and the depth of the chl a maximum (hatched band). The gray areas around the profiles show the 95% confidence intervals of the predictions. Confidence intervals are narrow for low concentrations and cannot always be visualized.

[29] The presented results show a clear relationship between PE concentrations and the spectral shape of L_u , especially for the data sets of the single cruises, thus corroborating the fact that PE influences the surrounding underwater light field, by absorption and scattering processes, and also by fluorescence emission. In order to focus on changes in spectral shape of the L_u spectra rather than magnitude, the spectra were standardized to minimize the component of variability due to spectral amplitude thus accounting for the inclusion of samples from different depths with different light availability. We tried the same analysis with nonstandardized data and got relatively poor model fits, compared to the standardized data set. *Craig et*

al. [2012] also used a type of spectral scaling in order to focus their analysis on shape rather than magnitude. They suggest that the use of normalized spectra emphasizes the color of the water carrying most of the information about chl a and phytoplankton absorption.

[30] The same analysis was conducted with flow cytometry data (i.e., cell counts of orange fluorescing cells and total orange fluorescence as measured by the flow cytometer) instead of PE data, but the relationships were not as strong as with the PE data. We suggest two possible reasons for the better performance with PE data:

[31] (1) Sample volume: The flow cytometry data are derived from measurements of very small sample volumes

(<0.0005 L) whereas for the PE measurements the sample volume was generally between 1 and 4 L. This large difference in sample volume could account for the fact that the L_u estimates provide a better fit to the PE data than to the cell counts.

[32] (2) Excitation wavelengths: From our own analysis of PE excitation spectra and other publications we know that the excitation of 488 nm used in the flow cytometric analysis is not optimal for all samples [e.g., *Olson et al.*, 1988]. Samples dominated by low-PUB species have their excitation maximum at ~ 550 nm, for no-PUB species this peak can even be shifted to 560 nm, whereas high-PUB species generally have two maxima at ~ 495 nm and at ~ 550 nm [*Hoge et al.*, 1998; *Lantoine and Neveux*, 1999; *Olson et al.*, 1988]. It has been demonstrated before [*Olson et al.*, 1988] that high-PUB cells show higher fluorescence when excited by a 488 nm laser than low-PUB cells. The low-fluorescence response of low- or no-PUB cells to the 488 nm laser of the flow cytometer might explain why some cells could be missed in this method, whereas the relative PE concentrations measured with the fluorometric technique are based on excitation scans ranging from 450 to 560 nm.

[33] Another fact that will add to the differences between flow cytometry and PE measurements, but also between PE and L_u measurements, is the species composition. Noteworthy species such as *Trichodesmium*, which form filaments and colonies, will probably not be detected in flow cytometry samples due to the size of the filaments and the small sample volume. There is a greater chance to encounter *Trichodesmium* filaments in a larger water sample, as was taken for the PE measurements; however, even the large Niskin bottles might miss the naturally buoyant colonies. Although we never detected any visible filaments on the sample filters or colonies in the surface waters, we cannot be sure that they were not present. The radiometer, however, would detect the spectral impact of a *Trichodesmium* bloom.

[34] For all data sets, EOF modes 1–3 explained between 98 and 99% of the total variance of standardized spectra. EOF mode 1 showed one main feature in the region of 400–500 nm probably due to chl *a* and other accessory pigments, while EOF mode 2 showed positive and negative spectral features in the same wavelength region, possibly due to a mixed effect of absorption and backscattering on the underwater light field. EOF mode 3 explained variation in the spectral region of 450–600 nm. As described in detail in the introduction, absorption spectra of PEs cover the spectral region of ~ 475 –580 nm (with absorption maxima at ~ 495 nm and ~ 545 nm for the PUB and PEB chromophores, respectively), and fluoresce at ~ 580 nm, depending on various factors such as taxonomy, pigment composition, light availability and nutrients [*Falkowski and Raven*, 1997; *Glazer and Stryer*, 1984; *Glazer et al.*, 1982; *Hoge et al.*, 1998; *Lantoine and Neveux*, 1999]. As a result of these spectral properties, we would expect that the presence or absence of PE would coincide with deviations in the L_u spectra in the spectral range of approximately 450–600 nm. This spectral region is generally known as the “green gap” as all other known photosynthetic pigments do not absorb or absorb only weakly in this region. Thus, we can assume that the interference from other pigments would be smallest

here. The spectral variability of PE in terms of the two chromophores PUB and PEB which absorb at ~ 495 nm and ~ 545 nm respectively will extend the influence of PE toward shorter wavelengths when high PUB-species are present, whereas no-PUB species would not influence the light spectrum below ~ 500 nm.

[35] As indicated by ΔAIC , the predictor that explained the variance in the data best was EOF coefficient 3, which explains the variance in the spectral region of 450–600 nm where we expect the main influence of PEs on the underwater light field, corroborating the validity of our model. The fact that we cannot explain the influence of PE on the L_u spectra by EOF mode 3 only, but also need to include other modes for a better correlation, is probably a function of the spectral variability of PEs and of the other pigments present in the cells. High-PUB PEs will have an impact on the underwater light field in the spectral region below 500 nm and the variance in this region is also described by EOF coefficients 1 and 2. The variability in the PUB/PEB ratio as well as the composition of accessory pigments could also be the reason that the number of EOF coefficients included in the models varies depending on the cruises which were included. It emphasizes the fact that the effect of PE on the underwater light field is apparent within a broad wavelength range and not only at the peaks of absorption or fluorescence.

[36] Using the GLMs based on EOFs, we could predict PE profiles based on radiance spectra for each station. Integrated values and seven example profiles are shown in Figure 4, with measured PE and the depth of the chl *a* maximum provided as reference. In open ocean regions, the PE signal can be linked to *Synechococcus* distribution patterns as published in the literature: *Synechococcus* is known to be more abundant in areas which are seasonally or permanently enriched with nutrients by strong upwelling or coastal inputs [*Olson et al.*, 1990; *Partensky et al.*, 1996, 1999; *Zubkov et al.*, 1998]. Highest integrated values are found in association with the Mauretania upwelling and off the coasts of Western Europe and South West Africa. At stations near the coast the detection of the marker pigment alloxanthin (pigment data not shown here) suggests the presence of cryptophytes which are probably responsible for the PE signal in these environments less typical for cyanobacteria.

[37] The predicted PE profiles generally reproduce the measured PE values well and the bands of 95% confidence intervals show the predictions to be robust. The GLM that we apply assumes a constant error across the range of measured PE concentrations. Translated to error as a percent of the concentration, the model is less sensitive in identifying variation at the lower range of PE concentrations and is more appropriate for identifying profile features at higher concentrations. The profiles show varying vertical distributions, which is not surprising as vertical profiles are influenced by numerous physico-chemical factors such as stability of the water column, light, temperature or nutrients, hence making it difficult to predict which profiles should be found in which region at a certain point in time. We often find that the PE-maximum is closely linked to the chl *a* maximum (see Figure A1 of the Appendix), a relationship that has been reported before [*Partensky et al.*, 1996]. However, exceptions exist where the PE maximum is located slightly

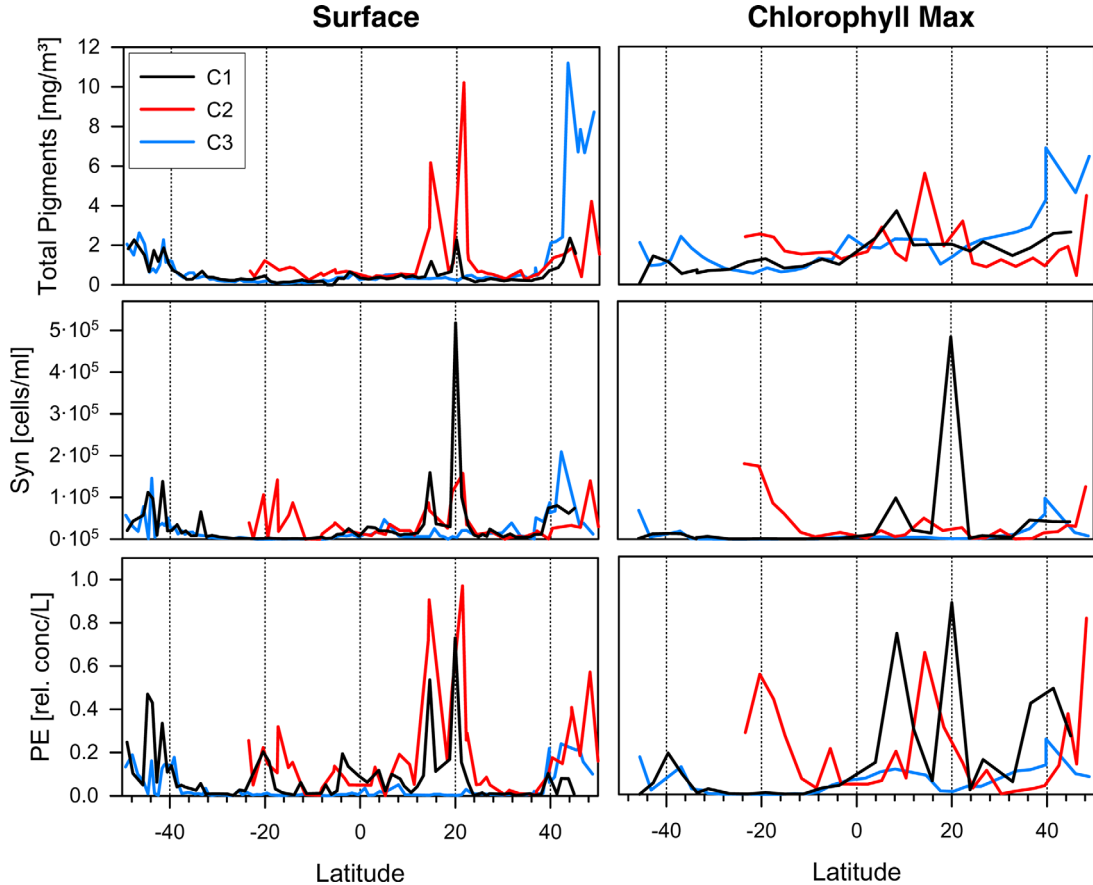


Figure 5. Concentrations of total pigments [mg/m^3] measured by HPLC, *Synechococcus* [cells/ml] measured by flow cytometry and PE [relative concentration/L] measured by a spectrofluorometric method by latitude. Each cruise is designated by color. Values are given for surface (left plots) and at the depth of the chl *a* maximum (right plots).

below the chl *a* maximum (for example profiles A and B in Figure 4). In some cases (as in profile C in Figure 4) there are two PE maxima and only one of them matches the chl *a* maximum. Profile F is an example where the PE maximum would have been missed entirely if samples had been taken only in the chl *a* maximum.

[38] The fact that we use relative PE concentrations limits our ability to compare with other PE quantifications. However, the aim of this study is not to show a distribution of absolute values of PE, but to demonstrate a method, which allows us to deduce PE values from radiometric measurements. The PE determination chosen as input parameter for the model dictates the output. Thus, should we or other laboratories have the possibility to quantify PE in absolute values, the output of the model would also be in absolute concentrations. However, purifying phycobiliproteins is not a straight forward procedure and, more importantly for the quantification of PEs, purified proteins often have different spectral properties than the proteins *in vivo*, as their spectral properties are strongly influenced by interactions in the complex assemblages of the phycobilisomes [Glazer, 1988].

[39] In our GLMs, we found the strongest relationship for the single cruise models and for the model with pooled data of C1+C2. However, the third cruise (C3), did not improve the correlation although within the cruise itself there was a strong relationship between L_u and PE measure-

ments. However, the range of relative PE concentrations of C3 was restricted to a much smaller range than in the two other cruises (0.001–0.25 relative units/L for C3, as opposed to 0.001–0.89 relative units/L and 0.001–0.72 relative units/L for C1 and C2, respectively). The cruises C1 and C2 were conducted on nearly the same cruise track and in the same season, with 2 years between them. To investigate possible reasons for these low-PE values, we looked at the pigment analysis and flow cytometry data of all three cruises (Figure 5). The amount of total pigment gives a general idea of the phytoplankton biomass present at each station and the flow cytometry data shown here gives the number of cells per milliliters of *Synechococcus* species, the most abundant phytoplankton with PE-containing phycobilisomes in open ocean waters. For comparison, the third plot in Figure 5 shows the measured PE concentration (relative units/L). Both C1 and C2 encountered major phytoplankton blooms with a high percentage of PE-containing phytoplankton in the Mauritanian upwelling, whereas C3 does not show any elevated pigment or PE levels at that latitude. C3 only encountered higher pigment concentration north of Spain and the percentage of PE-containing phytoplankton was very low in that area. These differences in pigment composition might explain why we obtain different models from the different cruises. They emphasize how important the input data are for the model output and how

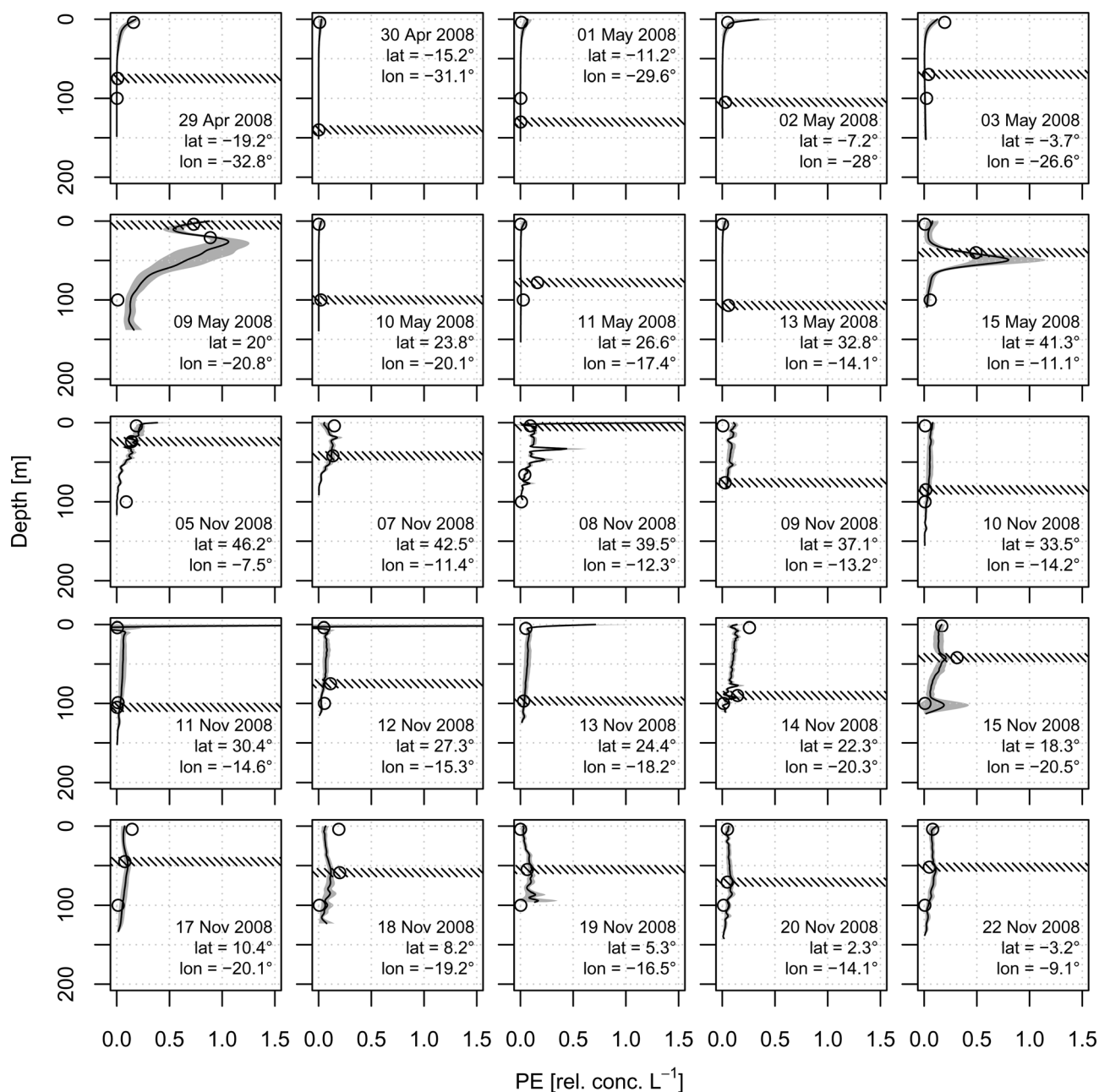


Figure A1. Predicted PE profiles for all stations, calculated with the single cruise models, including the values of measured PE (open circles) and the depth of the chl a maximum (hatched band). The gray areas around the profiles show the 95% confidence intervals of the predictions. Confidence intervals are narrow for low concentrations and cannot always be visualized.

crucial it is to have a broad set of data encompassing a wide range of pigment concentrations. Large interannual changes in (pico-) phytoplankton composition and dynamics have been reported previously [Dandonneau *et al.*, 2004; Head and Pepin, 2010a, 2010b; Partensky *et al.*, 1996] and should be taken into account.

5. Conclusions and Further Research

[40] We have developed a statistical approach to derive PE concentrations from underwater radiance measurements, which enables us to obtain a broader PE data set of

depth profiles than could be acquired through measurements of discrete water samples. We have shown that the influence that PE-containing phytoplankton has on the underwater light field can be exploited to calculate PE concentrations from L_u measurements. For any cruise or site where L_u and concurrent PE measurements are available, we can derive a model for PE estimation. There is still a need for discrete water samples for PE measurements as input and validation data for the model, but with our model, the resolution of the output data is much higher than it would ever be with discrete water samples and laboratory measurements.

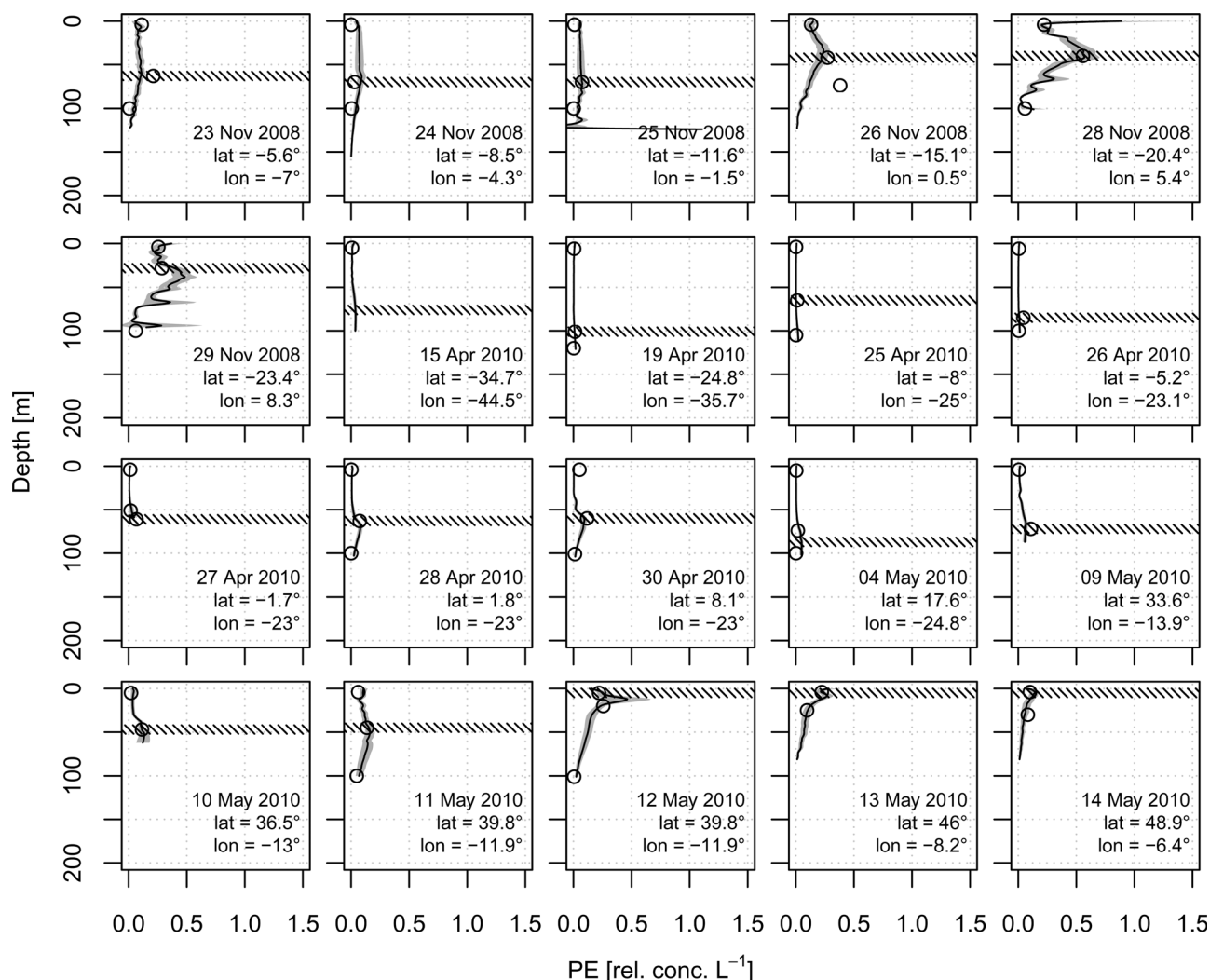


Figure A1. (continued)

[41] From our results, we conclude that, for the best approximation to reality, each cruise would need its own model to accommodate seasonal and interannual changes. Another possibility, which could be tested with more data, would be a separation of the data sets according to biogeographical regions or provinces instead of cruises and compare the model outcomes. We would also welcome a comparison of our model output with the output data set of specific PE sensors that are commercially available.

Appendix A

[42] Figure A1 shows calculated profiles of phycoerythrin (PE) distribution for all stations of the three cruises. Values of measured PE and the depth of the chlorophyll *a* (chl *a*) maximum are included for reference. We often find that the PE-maximum is closely linked to the chl *a* maximum.

[43] **Acknowledgments.** We would like to thank four anonymous reviewers for very helpful comments. We thank AWI, Helmholtz Impulse Fond (HGF Young Investigators Group Phytooptics) and OCEANET for funding. M.H.T. was supported by the German Research Foundation, project BiPhyCoSi (ID: LO-1143/6). We also thank the remote sensing group at the Helmholtz-Zentrum Geesthacht, Allan Cembella and his group at the

AWI as well as Oliver Zielinski and his group at the ICBM in Oldenburg for the use of their equipment. We are grateful to Erika Allhusen, Mirko Lunau, Anja Bernhardt and Sonja Wiegmann for help with the laboratory work and the crew, principal investigators and other scientists on board the RV Polarstern for support on board and fruitful discussions afterward.

References

- Algarra, P., M. Estrada, and F. X. Niell (1988), Phycobiliprotein distribution across the Western Mediterranean divergence, *Deep Sea Res. Part A*, 35(8), 1425–1430.
- Beutler, M., K. H. Wiltshire, B. Meyer, C. Moldaenke, C. Luring, M. Meyerhofer, U. P. Hansen, and H. Dau (2002), A fluorometric method for the differentiation of algal populations in vivo and in situ, *Photosynth. Res.*, 72(1), 39–53.
- Beutler, M., K. H. Wiltshire, C. Reineke, and U. P. Hansen (2004), Algorithms and practical fluorescence models of the photosynthetic apparatus of red cyanobacteria and Cryptophyta designed for the fluorescence detection of red cyanobacteria and cryptophytes, *Aquat. Microbial Ecol.*, 35(2), 115–129.
- Capone, D. G., J. P. Zehr, H. W. Paerl, B. Bergman, and E. J. Carpenter (1997), *Trichodesmium*, a globally significant marine cyanobacterium, *Science*, 276(5316), 1221–1229, doi:10.1126/science.276.5316.1221.
- Carr, N. G., and N. H. Mann (1994), The oceanic cyanobacterial picoplankton, in *The Molecular Biology of Cyanobacteria*, edited by D. A. Bryant, pp. 27–48, Kluwer Acad., Dordrecht.

- Chekalyuk, A. M., and M. Hafez (2008), Advanced laser fluorometry of natural aquatic environments, *Limnol. Oceanogr.*, 6, 591–609.
- Chekalyuk, A. M., M. R. Landry, R. Goericke, A. G. Taylor, and M. A. Hafez (2012), Laser fluorescence analysis of phytoplankton across a frontal zone in the California current ecosystem, *J. Plankton Res.*, 34(9), 761–777, doi:10.1093/plankt/fbs034.
- Clay, B. L., P. Kugrens, and R. E. Lee (1999), A revised classification of Cryptophyta, *Bot. J. Linnean Soc.*, 131(2), 131–151, doi:10.1111/j.1095-8339.1999.tb01845.x.
- Coble, P. G., C. A. Schultz, and K. Mopper (1993), Fluorescence contouring analysis of DOC intercalibration experiment samples—A comparison of techniques, *Mar. Chem.*, 41(1–3), 173–178, doi:10.1016/0304-4203(93)90116-6.
- Cole, K. M., and R. G. Sheath (Eds.) (1990), *Biology of the Red Algae*, Cambridge Univ. Press, Cambridge, U.K.
- Cowles, T. J., R. A. Desiderio, and S. Neuer (1993), In situ characterization of phytoplankton from vertical profiles of fluorescence emission-spectra, *Mar. Biol.*, 115(2), 217–222, doi:10.1007/Bf00346338.
- Craig, S. E., C. T. Jones, W. K. W. Li, G. Lazin, E. Horne, C. Caverhill, and J. J. Cullen (2012), Deriving optical metrics of coastal phytoplankton biomass from ocean colour, *Remote Sens. Environ.*, 119, 72–83, doi:10.1016/j.rse.2011.12.007.
- Dandonneau, Y., P. Y. Deschamps, J. M. Nicolas, H. Loisel, J. Blanchot, Y. Montel, F. Thieuleux, and G. Becu (2004), Seasonal and interannual variability of ocean color and composition of phytoplankton communities in the North Atlantic, equatorial Pacific and South Pacific, *Deep Sea Res. Part II*, 51(1–3), 303–318, doi:10.1016/j.dsr2.2003.07.018.
- Desiderio, R. A., C. Moore, C. Lantz, and T. J. Cowles (1997), Multiple excitation fluorometer for in situ oceanographic applications, *Appl. Optics*, 36(6), 1289–1296, doi:10.1364/Ao.36.001289.
- Downes, M. T., and J. A. Hall (1998), A sensitive fluorometric technique for the measurement of phycobilin pigments and its application to the study of marine and freshwater picophytoplankton in oligotrophic environments, *J. Appl. Phycol.*, 10(4), 357–363.
- Dubelaar, G. B. J., P. L. Gerritzen, A. E. R. Beeker, R. R. Jonker, and K. Tangen (1999), Design and first results of CytoBuoy: A wireless flow cytometer for in situ analysis of marine and fresh waters, *Cytometry*, 37(4), 247–254.
- Everroad, R. C., and A. M. Wood (2006), Comparative molecular evolution of newly discovered picocyanobacterial strains reveals a phylogenetically informative variable region of beta-phycoerythrin, *J. Phycol.*, 42(6), 1300–1311, doi:10.1111/j.1529-8817.2006.00282.x.
- Everroad, R. C., and A. M. Wood (2012), Phycoerythrin evolution and diversification of spectral phenotype in marine *Synechococcus* and related picocyanobacteria, *Mol. Phylogenet. Evol.*, 64(3), 381–392, doi:10.1016/j.ympev.2012.04.013.
- Falkowski, P. G., and J. A. Raven (1997), *Aquatic Photosynthesis*, Blackwell Sci, Malden, Massachusetts.
- French, C. S., and V. K. Young (1952), The fluorescence spectra of red algae and the transfer of energy from phycoerythrin to phycocyanin to chlorophyll, *J. Gen. Physiol.*, 35(6), 873–890.
- Gabrielson, P. W., D. J. Garbary, M. R. Sommerfeld, R. A. Townsend, and P. L. Tyler (1989), Phylum Rhodophyta, in *Handbook of Protoctista: The Structure, Cultivation, Habitats and Life Histories of the Eukaryotic Microorganisms and Their Descendants Exclusive of Animals, Plants and Fungi*, edited by L. Margulis, J. O. Corliss, M. Melkonian and D. J. Chapman, pp. 102–118, Jones and Barlett, Boston.
- Gantt, E., and S. F. Conti (1966), Phycobiliprotein Localization in Algae, *Brookhaven Symp. Biol.*, 19, 393–405.
- Gillot, M. (1989), Phylum Cryptophyta (Cryptomonads), in *Handbook of Protoctista: The Structure, Cultivation, Habitats and Life Histories of the Eukaryotic Microorganisms and Their Descendants Exclusive of Animals, Plants and Fungi*, edited by L. Margulis, J. O. Corliss, M. Melkonian, and D. J. Chapman, pp. 139–151, Jones and Barlett, Boston.
- Glazer, A. N. (1988), Phycobilisomes, *Methods Enzymol.*, 167, 304–312.
- Glazer, A. N. (1999), Cyanobacterial photosynthetic apparatus: An overview, in *Marine Cyanobacteria*, special issue 19, edited by L. Charpy and A. W. D. Larkum, pp. 419–430, Bull. de l'Inst. océanographique, Monaco.
- Glazer, A. N., and L. Stryer (1984), Phycofluor Probes, *Trends Biochem. Sci.*, 9(10), 423–427, doi:10.1016/0968-0004(84)90146-4.
- Glazer, A. N., J. A. West, and C. Chan (1982), Phycoerythrins as chemotaxonomic markers in red algae—A survey, *Biochem. Syst. Ecol.*, 10(3), 203–215.
- Gordon, H. R., D. K. Clark, J. L. Mueller, and W. A. Hovis (1980), Phytoplankton pigments from the Nimbus-7 coastal zone color scanner—Comparisons with surface measurements, *Science*, 210(4465), 63–66, doi:10.1126/science.210.4465.63.
- Haverkamp, T. H. A., D. Schouten, M. Doeleman, U. Wollenzien, J. Huisman, and L. J. Stal (2009), Colorful microdiversity of *Synechococcus* strains (picocyanobacteria) isolated from the Baltic Sea, *ISME J.*, 3(4), 397–408, doi:10.1038/ismej.2008.118.
- Head, E. J. H., and P. Pepin (2010a), Monitoring changes in phytoplankton abundance and composition in the Northwest Atlantic: A comparison of results obtained by continuous plankton recorder sampling and colour satellite imagery, *J. Plankton Res.*, 32(12), 1649–1660, doi:10.1093/plankt/fbq120.
- Head, E. J. H., and P. Pepin (2010b), Spatial and inter-decadal variability in plankton abundance and composition in the Northwest Atlantic (1958–2006), *J. Plankton Res.*, 32(12), 1633–1648, doi:10.1093/plankt/fbq090.
- Hill, D. R. A., and K. S. Rowan (1989), The biliproteins of the Cryptophyceae, *Phycologia*, 28(4), 455–463, doi:10.2216/i0031-8884-28-4-455.1.
- Hoef-Emden, K. (2008), Molecular phylogeny of phycocyanin-containing cryptophytes: Evolution of biliproteins and geographical distribution, *J. Phycol.*, 44(4), 985–993, doi:10.1111/j.1529-8817.2008.00530.x.
- Hoffmann, L. J., I. Peeken, K. Lochte, P. Assmy, and M. Veldhuis (2006), Different reactions of Southern Ocean phytoplankton size classes to iron fertilization, *Limnol. Oceanogr.*, 51(3), 1217–1229.
- Hoge, F. E., and R. N. Swift (1990), Photosynthetic Accessory Pigments - Evidence for the Influence of Phycoerythrin on the Submarine Light-Field, *Remote Sens. Environ.*, 34(1), 19–35.
- Hoge, F. E., C. W. Wright, T. M. Kana, R. N. Swift, and J. K. Yungel (1998), Spatial variability of oceanic phycoerythrin spectral types derived from airborne laser-induced fluorescence emissions, *Appl. Optics*, 37(21), 4744–4749, doi:10.1364/Ao.37.004744.
- Horiuchi, T., and F. Wolk (2008), Multispectral measurements of fluorescence and phytoplankton, *Sea Technol.*, 49(9), 15–19.
- Iturriaga, R., and B. G. Mitchell (1986), Chroococcoid cyanobacteria - a significant component in the food web dynamics of the open ocean, *Mar. Ecol. Prog. Ser.*, 28(3), 291–297, doi:10.3354/meps028291.
- Kim, J. J., Y. M. Jeon, J. H. Noh, and M. Y. Lee (2011), Isolation and characterization of a new phycoerythrin from the cyanobacterium *Synechococcus* sp. ECS-18, *J. Appl. Phycol.*, 23(1), 137–142, doi:10.1007/s10811-010-9554-2.
- Kirk, J. T. O. (1986), Optical properties of picoplankton suspensions, in *Photosynthetic Picoplankton*, edited by T. Platt and W. K. W. Li, vol. 214, pp. 501–520, Can. Bull. of Fish. and Aquat. Sci., Ottawa.
- Kronick, M. N. (1986), The use of phycobiliproteins as fluorescent labels in immunoassay, *J. Immunol. Methods*, 92(1), 1–13.
- Lantoine, F., and J. Neveux (1997), Spatial and seasonal variations in abundance and spectral characteristics of phycoerythrins in the tropical north-eastern Atlantic Ocean, *Deep Sea Res. Part I*, 44(2), 223–246.
- Lantoine, F., and J. Neveux (1999), Phycoerythrins in the sea: Abundance and spectral diversity, in *Marine Cyanobacteria*, special issue 19, edited by L. Charpy and A. W. D. Larkum, pp. 443–450, Bull. de l'Inst. océanographique, Monaco.
- Leboulanger, C., U. Dorigo, S. Jacquet, B. Le Berre, G. Paolini, and J. F. Humbert (2002), Application of a submersible spectrofluorometer for rapid monitoring of freshwater cyanobacterial blooms: A case study, *Aquat. Microb. Ecol.*, 30(1), 83–89, doi:10.3354/Ame030083.
- Lubac, B., and H. Loisel (2007), Variability and classification of remote sensing reflectance spectra in the eastern English Channel and southern North Sea, *Remote Sens. Environ.*, 110, 45–48.
- MacColl, R. (1998), Cyanobacterial phycobilisomes, *J. Struct. Biol.*, 124(2–3), 311–334, doi:10.1006/jsbi.1998.4062.
- Marie, D., N. Simon, and D. Vaultot (2005), Phytoplankton cell counting by flow cytometry, in *Algal Culturing Techniques*, edited by R. A. Andersen, pp. 253–268, Elsevier Acad. Press, Amsterdam.
- Matsuoka, A., Y. Hout, K. Shimada, S. Saitoh, and M. Babin (2007), Bio-optical characteristics of the western Arctic Ocean: Implications for ocean color algorithms, *Can. J. Remote Sens.*, 33(6), 503–518.
- McClain, C. R. (2009), A decade of satellite ocean color observations, *Annu. Rev. Mar. Sci.*, 1, 19–42, doi:10.1146/annurev.marine.010908.163650.
- Morel, A. (1997), Consequences of a *Synechococcus* bloom upon the optical properties of oceanic (case 1) waters, *Limnol. Oceanogr.*, 42(8), 1746–1754.
- Mueller, J. L. (1976), Ocean color spectra measured off Oregon coast—Characteristic vectors, *Appl. Optics*, 15(2), 394–402.

- Neveux, J., M. M. B. Tenorio, C. Dupouy, and T. A. Villareal (2006), Spectral diversity of phycoerythrins and diazotroph abundance in tropical waters, *Limnol. Oceanogr.*, *51*(4), 1689–1698.
- North, G. R., T. L. Bell, R. F. Cahalan, and F. J. Moeng (1982), Sampling Errors in the Estimation of Empirical Orthogonal Functions, *Mon. Weather Rev.*, *110*(7), 699–706.
- Olson, R. J., S. W. Chisholm, E. R. Zettler, and E. V. Armbrust (1988), Analysis of *Synechococcus* pigment types in the sea using single and dual beam flow cytometry, *Deep Sea Res. Part A*, *35*(3), 425–440, doi:10.1016/0198-0149(88)90019-2.
- Olson, R. J., S. W. Chisholm, E. R. Zettler, and E. V. Armbrust (1990), Pigments, size, and distribution of *Synechococcus* in the North Atlantic and Pacific Oceans, *Limnol. Oceanogr.*, *35*(1), 45–58.
- Olson, R. J., A. Shalapyonok, and H. M. Sosik (2003), An automated submersible flow cytometer for analyzing pico- and nanophytoplankton: FlowCytobot, *Deep Sea Res. Part I*, *50*(2), 301–315.
- Ong, L. J., and A. N. Glazer (1991), Phycoerythrins of marine unicellular cyanobacteria: 1. Bilin types and locations and energy-transfer pathways in *Synechococcus* spp phycoerythrins, *J. Biol. Chem.*, *266*(15), 9515–9527.
- Ong, L. J., A. N. Glazer, and J. B. Waterbury (1984), An unusual phycoerythrin from a marine Cyanobacterium, *Science*, *224*(4644), 80–83.
- Palenik, B. (2001), Chromatic adaptation in marine *Synechococcus* strains, *Appl. Environ. Microbiol.*, *67*(2), 991–994, doi:10.1128/aem.67.2.991-994.2001.
- Partensky, F., J. Blanchot, F. Lantoine, J. Neveux, and D. Marie (1996), Vertical structure of picophytoplankton at different trophic sites of the tropical northeastern Atlantic Ocean, *Deep Sea Res. Part I*, *43*(8), 1191–1213.
- Partensky, F., J. Blanchot, and D. Vaultot (1999), *Differential distribution and ecology of Prochlorococcus and Synechococcus in oceanic waters: A review*, in *Marine Cyanobacteria*, edited by L. Charpy and A. W. D. Larkum, vol. 19, pp. 457–475, Bull. de l'Inst. océanographique, Monaco.
- Proctor, C. W., and C. S. Roesler (2010), New insights on obtaining phytoplankton concentration and composition from in situ multispectral Chlorophyll fluorescence, *Limnol. Oceanogr.*, *8*, 695–708, doi:10.4319/lom.2010.8.695.
- R Development Core Team (2011), R: A Language and Environment for Statistical Computing. R Found. for Stat. Comput., Vienna, Austria, ISBN 3-900051-07-0. [Available at <http://www.R-project.org>, accessed 9 May 2013.]
- Scanlan, D. J., and N. J. West (2002), Molecular ecology of the marine cyanobacterial genera *Prochlorococcus* and *Synechococcus*, *FEMS Microbiol. Ecol.*, *40*(1), 1–12, doi:10.1016/s0168-6496(01)00217-3.
- Seppälä, J., P. Ylostalo, and H. Kuosa (2005), Spectral absorption and fluorescence characteristics of phytoplankton in different size fractions across a salinity gradient in the Baltic Sea, *Int. J. Remote Sens.*, *26*(2), 387–414, doi:10.1080/01431160410001723682.
- Sidler, W. A. (1994), Phycobilisome and Phycobiliprotein structures, in *The Molecular Biology of Cyanobacteria*, edited by D. A. Bryant, Kluwer Acad., Dordrecht.
- Six, C., J. C. Thomas, L. Garczarek, M. Ostrowski, A. Dufresne, N. Blot, D. J. Scanlan, and F. Partensky (2007), Diversity and evolution of phycobilisomes in marine *Synechococcus* spp.: A comparative genomics study, *Genome Biol.*, *8*(12), doi:10.1186/Gb-2007-8-12-R259.
- Smith, R. C., and K. S. Baker (1984), The analysis of ocean optical data, *Proc. Soc. Photo Opt. Instrum. Eng.*, *489*, 119–126.
- Staal, M., S. T. Hekkert, G. J. Brummer, M. Veldhuis, C. Sikkens, S. Persijn, and L. J. Stal (2007), Nitrogen fixation along a north-south transect in the eastern Atlantic Ocean, *Limnol. Oceanogr.*, *52*(4), 1305–1316, doi:10.4319/lo.2007.52.4.1305.
- Subramaniam, A., E. J. Carpenter, D. Karentz, and P. G. Falkowski (1999), Bio-optical properties of the marine diazotrophic cyanobacteria *Trichodesmium* spp. I. Absorption and photosynthetic action spectra, *Limnol. Oceanogr.*, *44*(3), 608–617.
- Taylor, B. B., E. Torrecilla, A. Bernhardt, M. H. Taylor, I. Peeken, R. Röttgers, J. Piera, and A. Bracher (2011), Bio-optical provinces in the eastern Atlantic Ocean and their biogeographical relevance, *Biogeosciences*, *8*(12), 3609–3629, doi:10.5194/bg-8-3609-2011.
- Toole, D. A., and D. A. Siegel (2001), Modes and mechanisms of ocean color variability in the Santa Barbara Channel, *J. Geophys. Res.*, *106*(C11), 26,985–27,000.
- Waterbury, J. B., and R. Rippka (1989), Subsection I. Order Chroococcales, in *Bergey's Manual of Systematic Bacteriology*, edited by J. T. Staley, M. P. Bryant, N. Pfennig and J. G. Holt, pp. 1728–1746, Williams & Wilkins, Baltimore, MD.
- Waterbury, J. B., S. W. Watson, R. R. L. Guillard, and L. E. Brand (1979), Widespread occurrence of a unicellular, marine, planktonic cyanobacterium, *Nature*, *277*(5694), 293–294, doi:10.1038/277293a0.
- Wood, A. M., D. A. Phinney, and C. S. Yentsch (1998), Water column transparency and the distribution of spectrally distinct forms of phycoerythrin-containing organisms, *Mar. Ecol. Prog. Ser.*, *162*, 25–31, doi:10.3354/Meps162025.
- Wyman, M. (1992), An in vivo method for the estimation of phycoerythrin concentrations in marine cyanobacteria (*Synechococcus* spp.), *Limnol. Oceanogr.*, *37*(6), 1300–1306.
- Wyman, M., R. P. F. Gregory, and N. G. Carr (1985), Novel role for phycoerythrin in a marine Cyanobacterium, *Synechococcus* strain DC2, *Science*, *230*(4727), 818–820, doi:10.1126/science.230.4727.818.
- Zhao, K.-H., R. J. Porra, and H. Scheer (2011), Phycobiliproteins, in *Phytoplankton Pigments—Characterization, Chemotaxonomy and Applications in Oceanography*, edited by S. Roy, C. A. Llewellyn, E. S. Egeland and G. Johnson, pp. 375–411 Cambridge Univ. Press, Cambridge.
- Zubkov, M. V., M. A. Sleight, G. A. Tarran, P. H. Burkill, and R. J. G. Leakey (1998), Picoplanktonic community structure on an Atlantic transect from 50 degrees N to 50 degrees S, *Deep Sea Res. Part I*, *45*(8), 1339–1355.